Available online at www.sciencedirect.com
SCIENCE DIRECT
Polymer 46 (2005) 3199–3209
polymer
www.elsevier.com/locate/polymer

Monodispersed thermoresponsive hydrogel microspheres with a volume phase transition driven by hydrogen bonding

Xin-Cai Xiao[1], Liang-Yin Chu*, Wen-Mei Chen, Jia-Hua Zhu

School of Chemical Engineering, Sichuan University, Chengdu, Sichuan 610065, China

Received 3 October 2004; received in revised form 8 January 2005; accepted 10 January 2005
Available online 5 March 2005

Abstract

We report the synthesis and characterization of monodispersed thermoresponsive hydrogel microspheres with a volume phase transition driven by hydrogen bonding. The prepared microspheres, composed of poly(acrylamide-*co*-styrene) (poly(AAM-*co*-St)) cores and poly(acrylamide)/poly(acrylic acid) (PAAM/PAAC) based interpenetrating polymer network (IPN) shells, were featured with high monodispersity and positively thermoresponsive volume phase transition characteristics with tunable swelling kinetics, i.e. the particle swelling was induced by an increase rather than a decrease in temperature. The monodisperse poly(AAM-*co*-St) seeds were prepared by emulsifier-free emulsion polymerization, the PAAM or poly(acrylamide-*co*-butyl methacrylate) (poly(AAM-*co*-BMA)) shells were fabricated on the seeds by free radical polymerization, and the core-shell microspheres with PAAM/PAAC based IPN shells were finished by a method of sequential IPN synthesis. The microsphere size increased with increasing both AAM and BMA dosages. The increase of hydrophilic monomer AAM dosage resulted in a better monodispersity, but the increase of hydrophobic monomer BMA dosage led to a worse monodispersity. With increasing the crosslinker methylenebisacrylamide (MBA) dosage, the mean diameter of the microspheres decreased and the monodispersity became better. An equimolar composition of AAC and AAM in the IPN shells of the microspheres resulted in a more complete shrinkage for the microspheres at temperatures lower than the upper critical solution temperature. Both BMA and MBA additions depressed the swelling ratio of the hydrodynamic diameter of the microspheres.

Keywords: Microspheres; Positively thermoresponsive; Monodispersity

1. Introduction

Environmental stimuli-responsive microgel particles are considered to be more effective than macroscopic gels for many potential applications, because microgel particles have a much higher interfacial area per unit mass of gel, which results in much greater exchange rates. The characteristic time of gel swelling has been reported to be proportional to the square of a linear dimension of the hydrogels [1]. Furthermore, microgel particles are readily packed in columns or used internally in the body. Recently, functional microspheres have been widely investigated [2–8] and a widespread attention has been paid to environmental stimuli-responsive polymeric hydrogel microspheres due to their potential applications in numerous fields [9–13], including controlled drug delivery [14–19], chemical separations [20,21], sensors [22–24], catalysis [25], and enzyme immobilization [26]. As there are many cases in which environmental temperature fluctuations occur naturally and the environmental temperature stimuli can be easily designed and artificially controlled, in recent years much attention has been focused on thermoresponsive gel microspheres [9–13,15,27–33]. Up to now, almost all of the thermoresponsive hydrogel microspheres have been featured with negatively thermoresponsive volume phase transition characteristics, i.e. the particles deswell with increasing environmental temperature, because most of them have been prepared with *N*-isopropylacrylamide [9–13,15,27–32]. The volume phase transitions of these gel microspheres in water have been observed that are driven by hydrophobic interactions between the macromolecules [34].

In the last decade, another kind of thermoresponsive

* Corresponding author. Tel.: +86 28 8546 0682; fax: +86 28 8540 4976.
E-mail address: chuly@scu.edu.cn (L.-Y. Chu).
[1] Present address: Department of Polymer Science, College of Chemistry and Molecule Science, Wuhan University, Wuhan, Hubei 430072, China.

0032-3861/$ - see front matter © 2005 Elsevier Ltd. All rights reserved.
doi:10.1016/j.polymer.2005.01.075

hydrogels has been reported that their volume phase transitions are driven by another type of interactions between the macromolecules, i.e. by hydrogen bonding [34–39]. The hydrogels are mainly composed of an interpenetrating polymer network (IPN) of poly(acrylamide) (PAAM) and poly(acrylic acid) (PAAC). Schematic illustration of the principle of hydrogen bonding-driven thermoresponsive volume phase transition in the PAAC/PAAM based IPN is shown in Fig. 1 [34,35,39]. The IPN hydrogels form intermolecular complexes via hydrogen bonding at temperatures lower than the upper critical solution temperature (UCST) while dissociate at temperatures higher than the UCST. Driven by the hydrogen bonding, the PAAM/PAAC based IPN hydrogels shrink at lower temperatures and swell at higher temperatures, revealing a positively thermoresponsive volume phase transition behavior which is opposite to that of poly(*N*-isopropylacrylamide). However, almost all of the previous investigations about the PAAM/PAAC based IPN hydrogels were focused on the macroscopic gels. Until very recently [33], little work has been reported on positively thermoresponsive microgel particles, although they should be preferred to negatively thermoresponsive microgels in certain applications.

On the other hand, morphology and monodispersity are very important for the stimuli-responsive microgel particles to improve their performance in various applications. For example, a uniform microsphere particle size is important for drug delivery systems, because the distribution of the microspheres within the body is greatly affected by the particle size [40]. In addition, if monodispersed microspheres are available, the drug release kinetics can be manipulated, thereby making it easier to formulate more sophisticated systems. A spherical shape of the microgel particles is also preferred for most of potential applications. However, there have not been any reports on the morphology and monodispersity of positively thermoresponsive microspheres.

The objective of the present work was to prepare monodisperse microspheres with positively thermoresponsive volume phase transition characteristics, i.e. the particles should be spherical and monodispersed, and the particle swelling should be induced by an increase rather than a decrease in temperature. This paper describes the synthesis and characterization of monodispersed core-shell thermoresponsive hydrogel microspheres with PAAM/-PAAC based IPN hydrogel shells, in which the volume phase transitions are driven by hydrogen bonding.

2. Experimental section

2.1. Materials

Acrylamide (AAM) and methylenebisacrylamide (MBA) were used after purifying by recrystallization in absolute ethyl alcohol and then drying in vacuo at room temperature. Acrylic acid (AAC), butyl methacrylate (BMA) and *N,N′*-dimethylformamide (DMF) were distilled under reduced pressure. Styrene (St) monomer was purified by 5 wt% NaOH, and then purified by vacuum distillation and stored in icebox. Potassium persulfate (KPS), which was used as a free radical initiator, was reagent grade and used as received without any further purification. Well-deionized and deoxygenated water, whose resistance was larger than 16 MΩ, was used in all the synthesis processes.

2.2. Preparation of core-shell microsphere seeds with poly(AAM-co-St) cores and PAAM or poly(AAM-co-BMA) shell layers

The preparation procedure of the core-shell microspheres is schematically illustrated in Fig. 2. In the first step, monodispersed poly(AAM-*co*-St) seeds were prepared by emulsifier-free emulsion polymerization. A mixture of AAM and St was dissolved in 165 mL of solvent in a 250-mL four-necked round-bottom flask equipped with a condenser, a nitrogen inlet, a thermometer and a stirrer. Nitrogen was bubbled into the solution and the mixture was stirred for 30 min at 550 rpm to remove oxygen from the monomeric phase. Polymerization was initiated by adding 15 mL of an aqueous solution containing KPS. The reaction was allowed to proceed for 2 h at 70 °C under stirring.

Then, keeping on the reaction by addition of AAM or AAM plus MBA, and the polymerization was continued for 22 h at 70 °C. In some cases, certain amount of hydrophobic monomer BMA was also added. In this second step, PAAM or poly(AAM-*co*-BMA) shells were fabricated on the microsphere seeds by free radical polymerization. The resulting monodisperse microspherical seeds, with

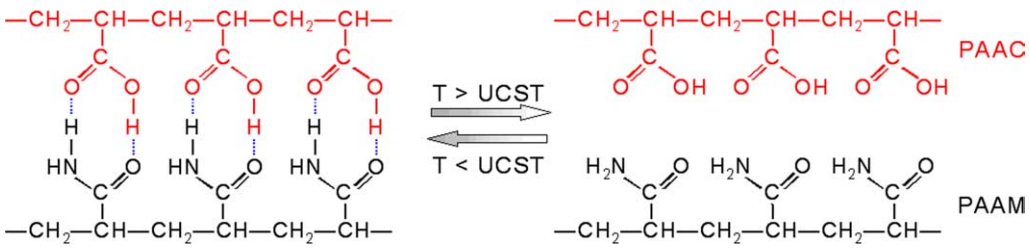

Fig. 1. Schematic illustration of the principle of thermoresponsive volume phase transition in the interpenetrating polymer network of poly(acrylic acid) and poly(acrylamide) driven by hydrogen bonding.

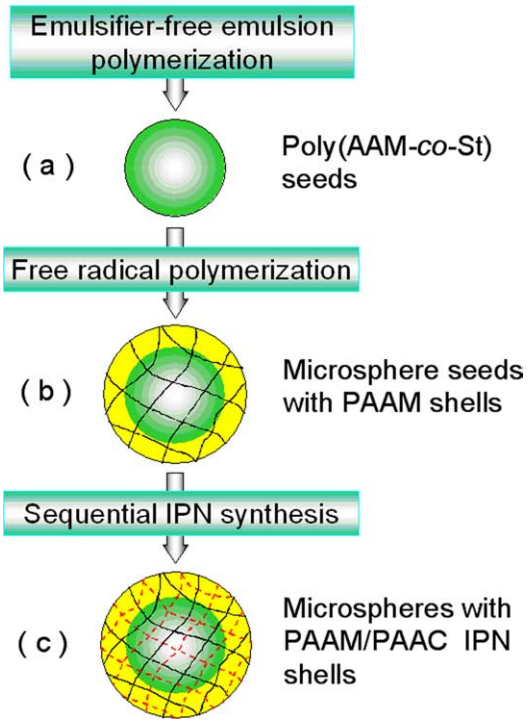

Fig. 2. Schematic illustration of the preparation procedure of the proposed positively thermoresponsive core-shell hydrogel microspheres.

poly(AAM-*co*-St) cores and PAAM or poly(AAM-*co*-BMA) shells, were dialyzed and purified by repetitive centrifugation, decantation, redispersion with well-deionized water, and then freeze-dried.

2.3. Preparation of core-shell microspheres with PAAM/PAAC based IPN shells

The core-shell microspheres with PAAM/PAAC based IPN shells were finished by a method of sequential IPN synthesis, in which microspheres with PAAM or poly(AAM-*co*-BMA) shells and PAAC gels were synthesized as initial matrix and as secondary gels, respectively. The seeds with PAAM or poly(AAM-*co*-BMA) shells were immerged in an aqueous AAC solution containing KPS and MBA as initiator and crosslinker, respectively. After the core-shell seeds swelling in the AAC solution for 24 h at 4 °C, the monomer AAC was subsequently polymerized and crosslinked within the initial core-shell seed matrixes for 24 h at 50 °C under nitrogen environment. The resulting microspheres were separated centrifugally, washed three times with deionized water, dialyzed against deionized water, and then freeze-dried.

2.4. Morphological analysis

SEM images of both freeze-dried seeds with PAAM or poly(AAM-*co*-BMA) shells and freeze-dried resulting microspheres with PAAM/PAAC based IPN shells were obtained using a scanning electron microscope (SEM; Hitachi S-450, Japan) at an accelerating voltage of 20 kV. Samples were mounted on a copper stub and sputter-coated with gold to minimize charging at fixed conditions (time 150 s, current 20 mA, voltage 2 kV).

2.5. Compositional analysis

To confirm the preparation of seeds with PAAM shells and the synthesis of microspheres with PAAM/PAAC based IPN shells, the seeds with PAAM shells and IPN microspheres were analyzed by Fourier transform infrared (FT-IR) spectroscopy using a KBr method (Nicolet MX-1E, USA).

2.6. Determination of the mean diameter and size distribution of the freeze-dried microspheres

The size distribution of freeze-dried microspheres was determined using a digital image analysis system on the basis of the SEM photographs of the microspheres. In the analysis, the particle number of each sample was always more than 300. In order to describe the monodispersity of microspheres quantitatively, an index named particle size dispersal coefficient, Span, was defined as

$$\text{Span} = \frac{D_{90} - D_{10}}{D_{50}} \quad (1)$$

Where D_n ($n = 10$, 50, and 90) denotes the cumulative number percentage of particles with diameter up to D_n is equal to $n\%$. The smaller the value of Span, the narrower the size distribution, i.e. the better the monodispersity. Usually, when the value of Span is smaller than 0.4, the particles could be taken as monodispersed [41,42].

2.7. Determination of thermoresponsive characteristics of the core-shell microspheres with PAAM/PAAC based IPN shells

The hydrodynamic diameters of the prepared core-shell hydrogel microspheres at different temperatures were determined by temperature-programmed photon correlation spectroscopy (TP-PCS; Brookhaven BI-9000AT, USA). This technique has been applied extensively to the characterization of such materials, as it allows for in situ size characterization of soft materials that cannot be reliably sized by electron microscopes due to deformation and/or dehydration under vacuum [10]. The dispersed particles in water were allowed to equilibrate thermally for 10–15 min before measurements were taken at each temperature. The hydrodynamic diameters of particles were calculated from diffusion coefficients by the Stokes–Einstein equation, and all correlogram analyses were performed using the manufacturer-supplied software. In the data presented in this study, each data point at a given temperature represents the

average valve of 15–20 measurements, with a 20 s integration time for each measurement.

To quantitively evaluate the swelling ratio of the microspheres at temperatures above the upper critical solution temperature (UCST) to that below the UCST, a swelling ratio of the hydrodynamic diameter at 40 °C to that at 10 °C was introduced as

$$\text{Swelling ratio} = \frac{d_{40}}{d_{10}} \quad (2)$$

Where d_{40} and d_{10} are hydrodynamic diameters of the microspheres at 40 and 10 °C, respectively.

3. Results and discussion

3.1. Morphology and monodispersity of microsphere seeds with poly(AAM-co-St) cores and PAAM or poly(AAM-co-BMA) shell layers

The morphology and monodispersity of the prepared microspheres with PAAM/PAAC based IPN shells are principally dependent on those of the seeds. Therefore, it is very important and essential to investigate the morphology and monodispersity of microsphere seeds with poly(AAM-*co*-St) cores and PAAM or poly(AAM-*co*-BMA) shell layers.

Fig. 3 shows the morphological characteristics of poly(AAM-*co*-St) microsphere seeds with PAAM shells prepared with different AAM dosages in the free radical polymerization step. Fig. 3(a)–(d) show the SEM micrographs of the seeds prepared with 0.5, 1.0, 1.5 and 2.0 g of AAM, respectively, and Figure 3(e) illustrates the effect of the AAM dosage on the mean diameter and monodispersity of the seeds. The SEM micrographs show that all of the seeds were satisfactorily spherical. The Span coefficients of the microsphere seeds in all of the cases were always less than 0.3, i.e. the seeds were monodispersed. With increasing the AAM dosage in the preparation of the PAAM shell layer, the mean diameter of microspheres increased; meanwhile the monodispersity became better slightly. The PAAM shell layers were fabricated on the poly(AAM-*co*-St) core seeds by a free radical polymerization method. By this method, the reaction manner was in graft polymerization because of some living radicals on the surfaces of polymerizing core particles. Because the number of core seeds per unit volume was constant, and monomer AAM contributed only to the PAAM shell formation on the seeds, therefore the mean diameters of the core-shell microsphere products became larger simply with increasing the AAM dosage. On the other hand, the free radical density of smaller particles was larger relatively, which was helpful for the smaller particles to absorb more monomers or polymers with low molecular weight onto their surfaces to form larger particles. Therefore, with increasing the AAM dosage, the monodispersity of the core-shell microspheres became better.

Fig. 4 shows the morphological characteristics of the microsphere seeds with poly(AAM*co*-BMA) shells prepared with different BMA dosages in the free radical polymerization. Fig. 4(a)–(d) illustrate the SEM micrographs and Fig. 4(e) shows the effect of BMA dosage on the mean diameter and monodispersity. With increasing the dosage of hydrophobic monomer BMA, the mean diameter of microsphere seeds increased, and the monodispersity became worse slightly. The increment of BMA dosage was not only beneficial to the particle growth, but also resulted in an increase of the number of colloidal droplets, i.e. the chances for forming small polymeric nucleus increased; therefore, the particle size dispersal coefficient became larger slightly as a result.

Fig. 5 illustrates the morphological characteristics of the poly(AAM-*co*-St) microsphere seeds with PAAM shells prepared with different MBA dosages in the free radical polymerization step. Fig. 5(a)–(d) show the SEM micrographs and Fig. 5(e) illustrates the effect of MBA dosage on the mean diameter and monodispersity. With increasing the dosage of crosslinker MBA, the mean diameter of the seeds decreased, and the particle size dispersal coefficient became smaller at the same time, i.e. monodispersity became better. The increment of crosslinking density of the shell layers of the seeds, which was resulted from the increase of crosslinker MBA dosage, hindered the diffusion of monomers into the nucleus; therefore prevented the seeds from growing. The larger the crosslinker MBA dosage, the more serious the hindrance, and then the smaller of the final size of the seeds. Meanwhile, with increasing the crosslinker MBA dosage, the chance of nucleation by the intertwining of polymer chains increased, and the nucleation time shortened.

In the subsequent growth stage, because the ratio of surface area to volume was larger for smaller particles, it was possible for the smaller particles to absorb more monomer. As a result, the growth rate of smaller particles was faster than that of larger ones. Therefore, the particle size trended to be uniform in the system finally, i.e. the monodispersity of the prepared microspheres became better.

3.2. Morphological comparison between the poly(AAM-co-St) seeds with PAAM shells and the microspheres with PAAM/PAAC based IPN shells

Fig. 6 shows SEM images of the poly(AAM-*co*-St) seeds with PAAM shells and the corresponding microspheres with PAAM/PAAC based IPN shells, from which it can be seen that both the core-shell seeds and the resulting IPN microspheres are highly monodisperse. The results in Fig. 6 show that the appearances, the particle size distributions and the mean diameters of the IPN microspheres were almost the same as those of the corresponding coreshell seeds. Because the seeds with PAAM shells were the initial

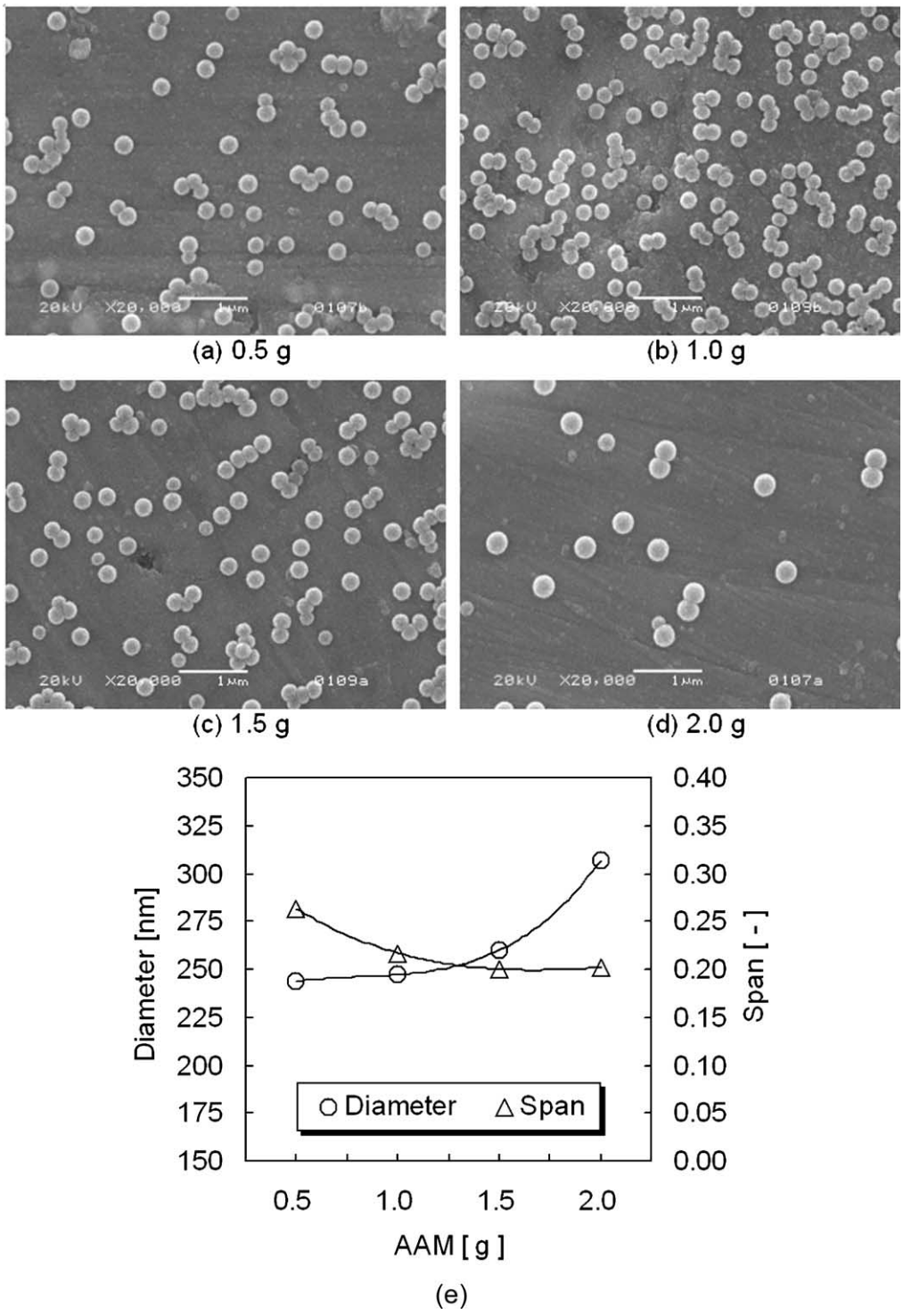

Fig. 3. Morphological characteristics of poly(AAM-*co*-St) microsphere seeds with PAAM shells prepared with different AAM dosages in the free radical polymerization. (a, b, c and d) SEM micrographs of the seeds prepared with 0.5, 1.0, 1.5 and 2.0 g of AAM, respectively. Scale bar 1 μm. (e) Effect of AAM dosage on the mean diameter and monodispersity of the seeds.

matrix for the IPN synthesis, the morphology and monodispersity of the final IPN microspheres were proven to be dependent on those of the core-shell seeds consequently.

Fig. 7 shows the KBr FT-IR spectra of the poly(AAM-*co*-St) seeds with PAAM shells, pure PAAC gels and microspheres with PAAM/PAAC based IPN shells, in which the IR spectra for carbonyl stretching regions for pure PAAM, pure PAAC and mixed PAAM/PAAC blends are compared. Carbonyl stretching resonances for pure systems of PAAM and PAAC are observed at 1671 and

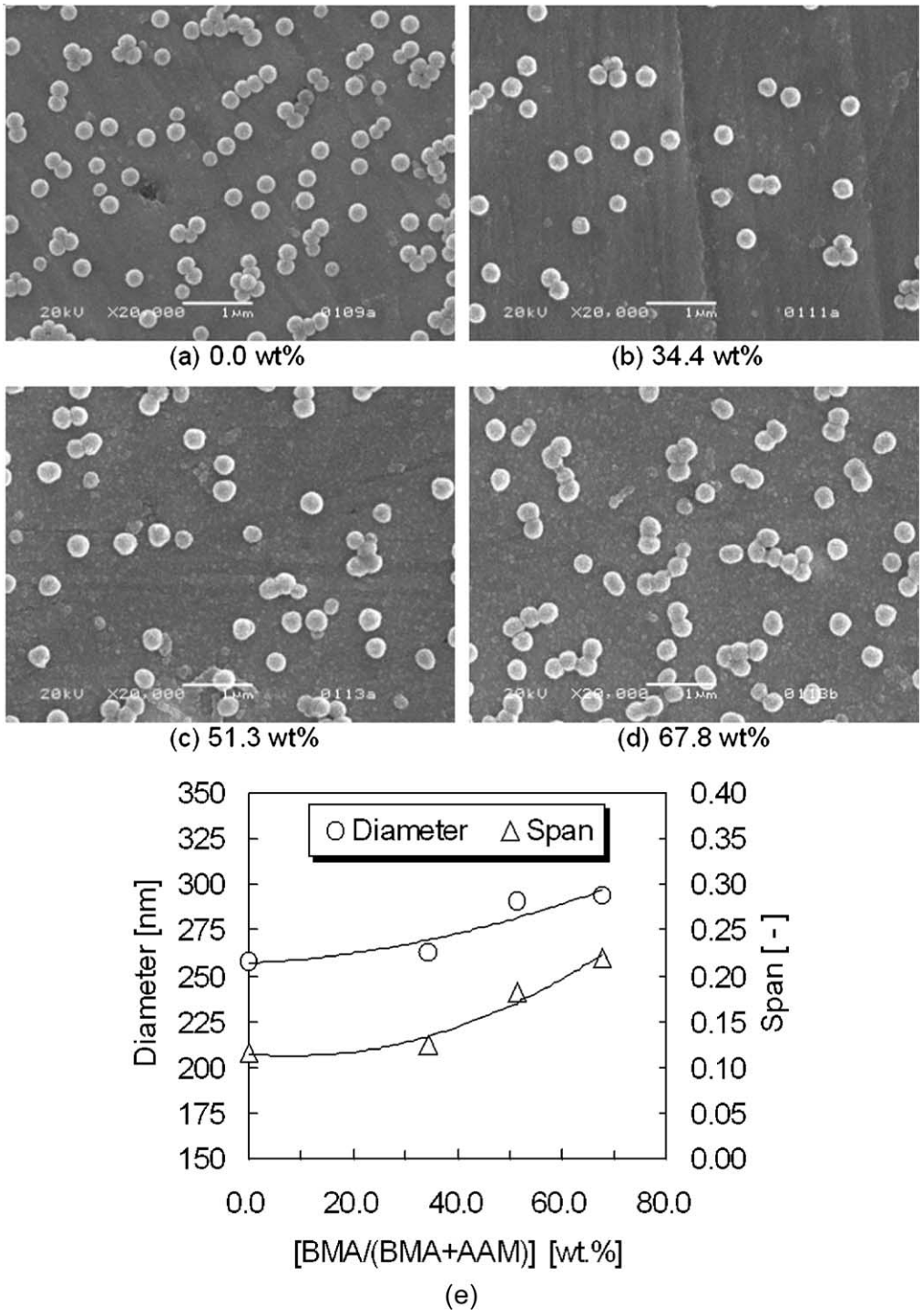

Fig. 4. Morphological characteristics of poly(AAM-*co*-St) microsphere seeds with poly(AAM-*co*-BMA) shells prepared with different BMA dosages in the free radical polymerization. (a, b, c and d) SEM micrographs of the seeds prepared with 0.0, 34.4, 51.3 and 67.8 wt% of [BMA]/([BMA]+[AAM]), respectively. Scale bar 1 μm. (e) Effect of BMA dosage on the mean diameter and monodispersity of the seeds.

1715 cm^{-1}, respectively. A distinctly different absorption band at 1664 cm^{-1} is observed for the PAAM/PAAC blends, attributed to PAAM carbonyl groups involved in hydrogen-bonded complexes, and a distinct absorption band at 1719 cm^{-1} is also observed for the PAAM/PAAC based IPN microspheres. These experimental observations confirm the PAAM/PAAC IPN synthesis in the preparation of microspheres, i.e. the prepared microspheres are proven to be constructed with PAAM/PAAC based IPN architecture.

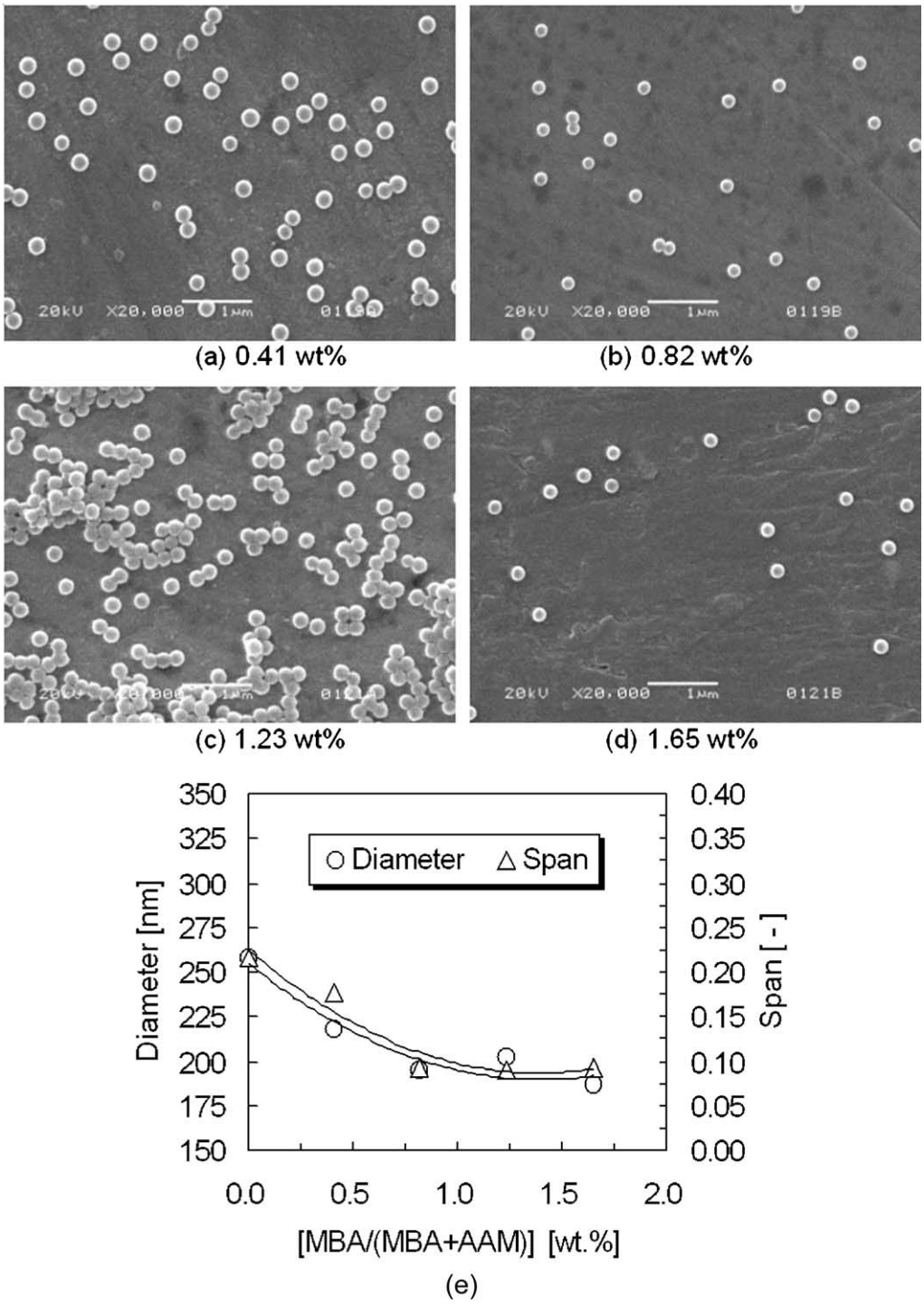

Fig. 5. Morphological characteristics of poly(AAM-*co*-St) microsphere seeds with PAAM shells prepared with different MBA dosages in the free radical polymerization. (a, b, c and d) SEM micrographs of the seeds prepared with 0.41, 0.82, 1.23 and 1.65 wt% of [MBA]/([MBA]+[AAM]), respectively. Scale bar 1 μm. (e) Effect of MBA dosage on the mean diameter and monodispersity of the seeds.

3.3. Thermoresponsive swelling characteristics of the core-shell microspheres with PAAM/PAAC based IPN shells

The temperature dependence of hydrodynamic diameter of the prepared microspheres with PAAM/PAAC based IPN shells is shown in Fig. 8, in which the microspheres exhibits a positively thermoresponsive volume phase transition behavior. The hydrodynamic diameters of the microspheres were about 215 nm in the temperature range from 10 to 15 °C, and increased to 370–380 nm in the temperature range from 30 to 40 °C. A sharp transition of the hydrodynamic diameters occurred on going from 15 to

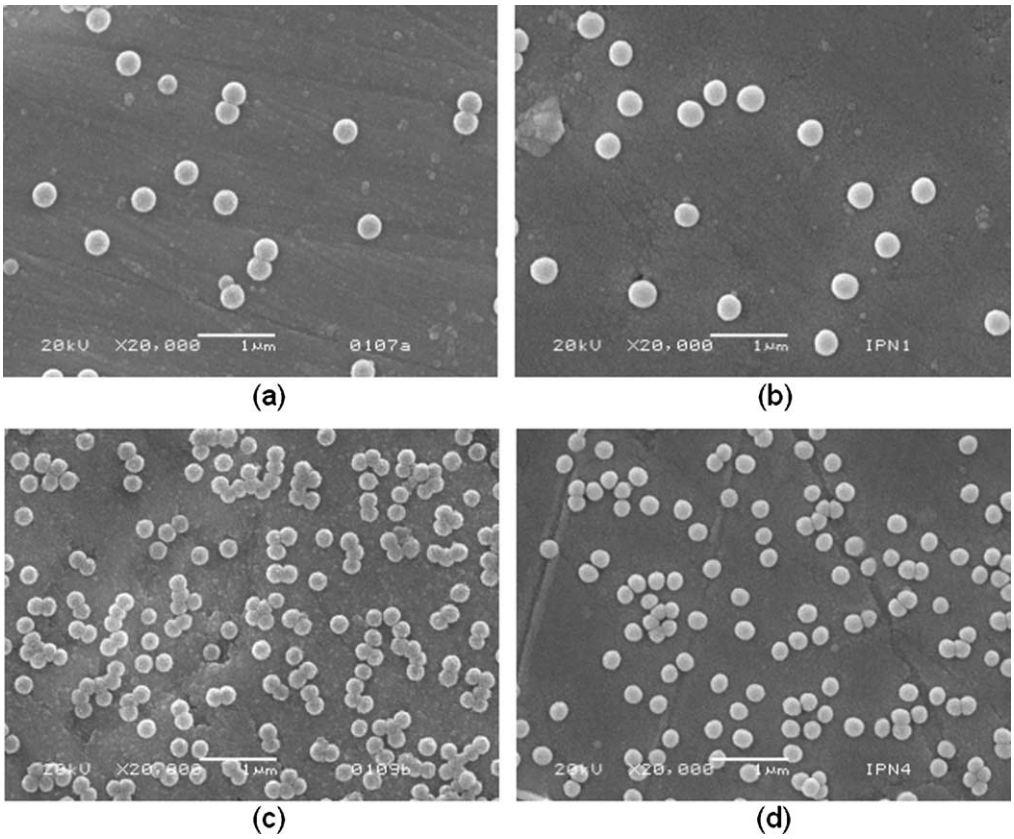

Fig. 6. SEM micrographs of poly(AAM-*co*-St) seeds with PAAM shells and the resulting microspheres with PAAM/PAAC based IPN shells. (a, c) seeds, (b, d) corresponding microspheres. (a, b) [AAM] = 2.0 g in the preparation of PAAM shells on seed cores (the second-step), (c, d) [AAM] = 1.0 g. Scale bar 1 μm.

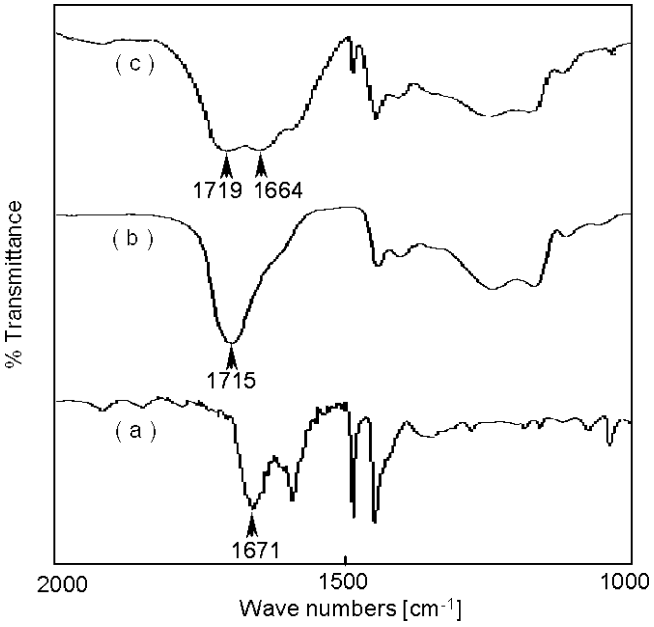

Fig. 7. KBr FT-IR spectra of (a) poly(AAM-*co*-St) seeds with PAAM shells, (b) poly(acrylic acid) and (c) microspheres with PAAM/PAAC based IPN shells.

25 °C, which corresponded to the UCST of PAAM/PAAC based IPN hydrogels [34–39]. Below the UCST, PAAM/PAAC intermolecular complexes formed by hydrogen bonding, and the chain–chain zipper effect made the IPN

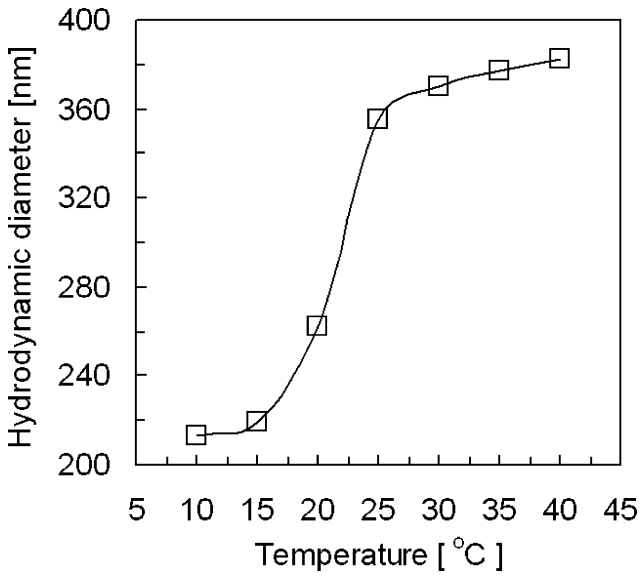

Fig. 8. Temperature-induced volume phase transition behavior of the core-shell microspheres with PAAM/PAAC based IPN shells. No BMA and MBA were added in the fabrication of PAAM shells on seed cores.

layers shrunken, as a result the mean hydrodynamic diameter was small. In contrast, the IPN microspheres were in the swollen state at temperatures above the UCST due to PAAM/PAAC complex dissociation by the breakage of hydrogen bonds, therefore resulting a larger hydrodynamic diameter.

Fig. 9 shows the effect of the AAC molar fraction of (AAC + AAM) in the IPN shells of the microspheres on the hydrodynamic diameters at 10 °C in deionized water. The curve displayed a minimum hydrodynamic diameter at 0.5 molar fraction of AAC. This result suggested that the PAAM/PAAC complex formed more strongly when the AAC molar fraction was equal to the AAM molar fraction in the IPN shell layer. The strong shrinkage of the IPN shells at 0.5 molar fraction of AAC at temperatures lower than the UCST was due to the precipitation of equimolar PAAM/PAAC hydrogen bonding polymer complexes. At other AAC molar ratios, the hydrodynamic diameter of the microspheres increased as AAC fraction shifted away from 0.5 to 0 or 1. Fig. 10 shows the effect of AAM dosage in the PAAM shell fabrication on the swelling ratio of hydrodynamic diameter of microspheres at 40 °C to that at 10 °C. The result presented a maximum swelling ratio of the hydrodynamic diameter for the microspheres prepared with a moderate AAM dosage in the PAAM shell fabrication. Either less or more AAM dosage resulted in smaller swelling ratios of the hydrodynamic diameters. When the AAM dosage was small in the fabrication of shells on the seeds, a thin shell layer was resulted; therefore the swelling-shrinkage degree of the core-shell particle was limited. With increasing the AAM dosage, the thickness of the fabricated shell layer increased, resulting in an increase of the swelling ratio of hydrodynamic diameter. However, when the AAM dosage increased too much, a very thick PAAM shell layer was resulted, making it difficult for crosslinked PAAC polymers formed throughout the whole shell layer in the IPN fabrication, i.e. it became difficult to achieve equimolar composition of AAC and AAM in the IPN shells.

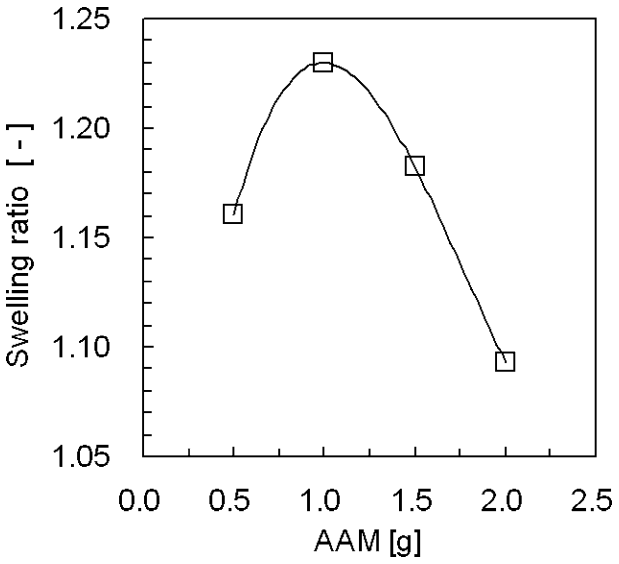

Fig. 10. Effect of AAM dosage in the PAAM shell fabrication on the swelling ratio of hydrodynamic diameters of core-shell microspheres at 40 °C to that at 10 °C.

Fig. 11 illustrates the effect of BMA and MBA additions in the PAAM shell preparation on the swelling ratio of hydrodynamic diameters of the microspheres at 40 °C to that at 10 °C. By comparing sample No. 1 with sample

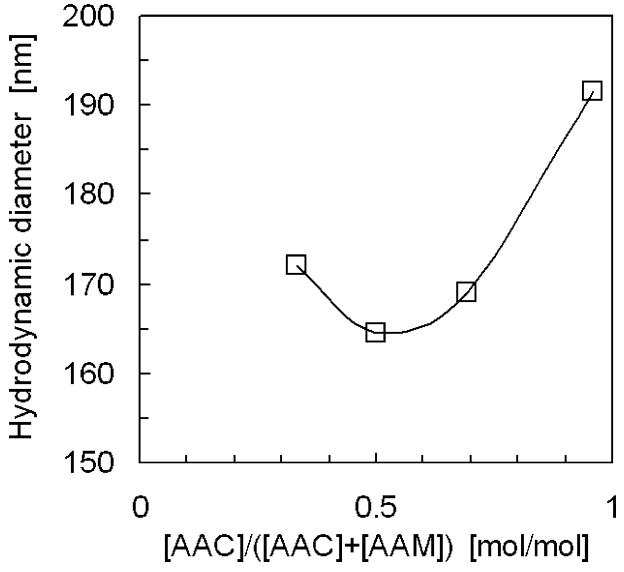

Fig. 9. Effect of the AAC molar fraction of (AAC + AAM) in the IPN shells on the hydrodynamic diameters of core-shell microspheres at 10 °C in deionized water.

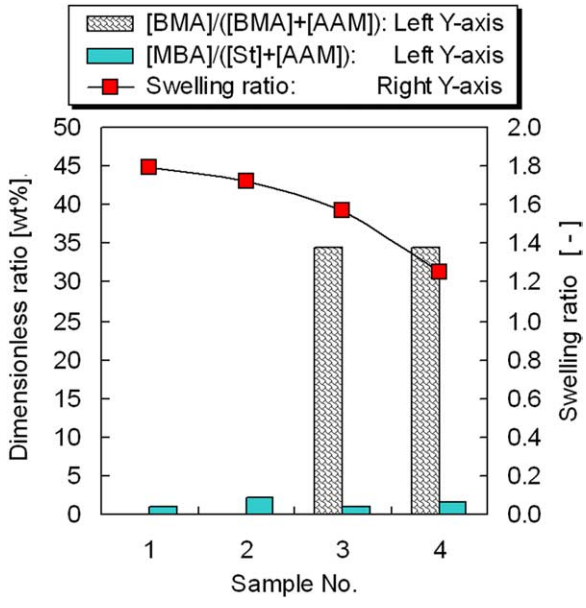

Fig. 11. Effect of BMA and MBA additions in the PAAM shell preparation on the swelling ratio of hydrodynamic diameters of core-shell microspheres at 40 °C to that at 10 °C.

No. 3, it was found that the swelling ratios of the hydrodynamic diameters of IPN microspheres decreased when adding BMA into the experimental recipe for the preparation of PAAM shells. The hydrophobic monomer BMA has been reported to contribute to the mechanical properties of the PAAM/PAAC based IPN macroscopic IPNs [35], the increase in the mechanical strength of the IPN shell restricted the swelling and shrinkage of the microspheres. In addition, hydrophobic interactions have been proposed to increase with increasing BMA content in the IPNs [35,37]. The hydrophobic interactions prevented the polymer chain complexes from dissociating, i.e. stabilized the hydrogen bonding complexation of the PAAM/PAAC based IPNs. By comparing sample No. 1 with sample No. 2 or sample No. 3 with sample No. 4, the results showed that the swelling ratio of the hydrodynamic diameters of microspheres also decreased to some extents with increasing crosslinker MBA dosage. By adding crosslinker MBA in the PAAM shell preparation or increasing MBA dosage in the IPN synthesis, the network of PAAM chains or that of PAAC chains became more rigid and the polymer chains restricted to each other more strongly, therefore the deformation of the IPN shells became more difficult. As a result, the swelling ratio of the hydrodynamic diameter of the microspheres was depressed. The results indicated that the swelling ratio of the microspheres could be adjusted by regulating the hydrophobic monomer BMA dosage and the crosslinker MBA dosage in the preparation.

4. Conclusions

The morphology, monodispersity and thermoresponsive swelling characteristics of coreshell PAAM/PAAC based IPN hydrogel microspheres with a volume phase transition driven by hydrogen bonding have been investigated systematically. The microspheres were featured with satisfactory monodispersity and positively thermoresponsive volume phase transition characteristics with tunable swelling kinetics, i.e. the particle swelling was induced by an increase rather than a decrease in temperature. With increasing monomer AAM dosage in the PAAM shell preparation, the diameter of microspheres increased and the monodispersity became better. With increasing hydrophobic monomer BMA dosage, the mean diameter of microspheres increased while the monodispersity became worse. With increasing crosslinker MBA dosage, the microsphere size decreased and the monodispersity became better. An equimolar composition of AAC and AAM in the IPN shells resulted in a more complete shrinkage for the microspheres at temperatures lower than the UCST. The swelling ratios of the hydrodynamic diameters of microspheres decreased when adding hydrophobic monomer BMA and/or crosslinker MBA into the experimental recipe for the preparation of the functional shells of the microspheres.

Acknowledgements

This work was financially supported by the National Natural Science Foundation of China (Grant No. 20206019), the Trans-Century Training Programme Foundation for the Talents by the Ministry of Education of China (Grant No. 2002-48), and Sichuan Youth Science and Technology Foundation for Distinguished Young Scholars (Grant No. 03ZQ026-41). The authors gratefully acknowledge the help of Dr Xu-Hong Peng in Lanzhou University for the hydrodynamic diameter measurements by TP-PCS.

References

[1] Tanaka T, Fillmore DJ. J Chem Phys 1979;70:1214–8.
[2] Lee IS, Cho MS, Choi HJ. Polymer 2005;46:1317–21.
[3] Kim JW, Lee JE, Kim SJ, Lee JS, Ryu JH, Kim J, et al. Polymer 2004; 45:4741–7.
[4] Kimura K, Kohama S, Yamashita Y, Uchida T, Sakaguchi Y. Polymer 2003;44:7383–7.
[5] Chen X, Cui Z, Chen Z, Zhang K, Lu G, Zhang G, et al. Polymer 2002; 43:4147–52.
[6] Lee MG. Polymer 2002;43:4307–9.
[7] Sandor M, Bailey NA, Mathiowitz E. Polymer 2002;43:279–88.
[8] Sosnowski S. Polymer 2001;42:637–43.
[9] Pelton R. Adv Colloid Interface Sci 2000;85:1–23.
[10] Gan D, Lyon LA. J Am Chem Soc 2001;123:7511–7.
[11] Gan D, Lyon LA. J Am Chem Soc 2001;123:8203–9.
[12] Jones CD, Lyon LA. Macromolecules 2000;33:8301–6.
[13] Jones CD, Lyon LA. Macromolecules 2003;36:1988–93.
[14] Kwon IC, Bae YH, Kim SW. Nature 1991;354:291–3.
[15] Ichikawa H, Fukumori Y. J Controlled Release 2000;63:107–19.
[16] Jeong B, Bae YH, Lee DS, Kim SW. Nature 1997;388:860–2.
[17] Leobandung W, Ichikawa H, Fukumori Y, Peppas NA. J Appl Polym Sci 2003;87:1678–84.
[18] Murthy N, Thng YX, Schuck S, Xu MC, Frechet JMJ. J Am Chem Soc 2002;124:12398–9.
[19] Vihola H, Laukkanen A, Hirvonen J, Tenhu H. Eur J Pharm Sci 2002; 16:69–74.
[20] Kawaguchi H, Fujimoto K. Bioseparation 1998;7:253–8.
[21] Kondo A, Kaneko T, Higashitani K. Biotechnol Bioeng 1994;44:1–6.
[22] Hu ZB, Chen YY, Wang CJ, Zheng YD, Li Y. Nature 1998;393: 149–52.
[23] Panchapakesan B, DeVoe DL, Widmaier MR. Nanotechnology 2001; 12:336–49.
[24] van der Linden H, Herber S, Olthuis W. Sensor Mater 2002;14: 129–35.
[25] Bergbreiter DE, Case BL, Liu Y-S, Waraway JW. Macromolecules 1998;31:6053–62.
[26] Guiseppi-Elie A, Sheppard NF, Brahim S, Narinesingh D. Biotechnol Bioeng 2001;75:475–84.
[27] Matsuoka H, Fujimoto K, Kawaguchi H. Polym Gels Networks 1998; 6:319–32.
[28] Matsuoka H, Fujimoto K, Kawaguchi H. Polym J 1999;31:1139–44.
[29] Zhu PW, Napper DH. Langmuir 2000;16:8543–5.
[30] Varga I, Gilanyi T, Meszaros R, Filipcsei G, Zrinyi M. J Phys Chem B 2001;105:9071–6.
[31] Gao J, Hu Z. Langmuir 2002;18:1360–7.
[32] Zha L, Zhang Y, Yang W, Fu S. Adv Mater 2002;14:1090–2.
[33] Bouillot P, Vincent B. Colloid Polym Sci 2000;278:74–9.
[34] Ilmain F, Tanaka T, Kokufuta E. Nature 1991;349:400–1.

[35] Katono H, Maruyama A, Sanui K, Ogata N, Okano T, Sakurai Y. J Controlled Release 1991;16:215–28.
[36] Katono H, Sanui K, Ogata N, Okano T, Sakurai Y. Polym J 1991;23: 1179–89.
[37] Sasase H, Aoki T, Katona K, Sanui K, Ogata N, Ohta R, et al. Makromol Chem Rapid Commun 1992;13:577–81.
[38] Aoki T, Kawashima M, Katono H, Sanui K, Ogata N, Okano T, et al. Macromolecules 1994;27:947–52.
[39] Endo N, Shirota H, Horie K. Macromol Rapid Commun 2001;22: 593–7.
[40] Shiga K, Muramatsu N, Kondo T. J Pharm Pharmacol 1996;48:891–5.
[41] Chu LY, Xie R, Zhu JH, Chen WM, Yamaguchi T, Nakao S. J Colloid Interface Sci 2003;265:187–96.
[42] Chu LY, Park SH, Yamaguchi T, Nakao S. Langmuir 2002;18: 1856–64.